Inorg. Chem. **2002**, *41*, 2266–2274

Inorganic Chemistry
Article

Kinetics and Mechanism of Rhenium-Catalyzed Oxygen Atom Transfer from Pyridine *N*-Oxides to Phosphines

Ying Wang and James H. Espenson*

Ames Laboratory and Department of Chemistry, Iowa State University of Science and Technology, Ames, Iowa 50011

Received December 20, 2001

The oxygen atom transfer (OAT) reaction cited does not occur on its own in >10 h. Oxorhenium(V) compounds having the formula MeReO(dithiolate)PZ_3 catalyze the reaction; the catalyst most studied was MeReO(mtp)PPh_3, **1**, where mtpH_2 = 2-(mercaptomethyl)thiophenol. The mechanism was studied by multiple techniques. Kinetics (initial-rate and full-time-course methods) established this rate law: $v = k_c[\mathbf{1}][\mathrm{PyO}]^2[\mathrm{PPh_3}]^{-1}$. Here and elsewhere PyO symbolizes the general case XC_5H_4NO and PicO that with X = 4-Me. For 4-picoline, $k_c = (1.50 \pm 0.05) \times 10^4$ L mol^{-1} s^{-1} in benzene at 25.0 °C; the inverse phosphine dependence signals the need for the removal of phosphine from the coordination sphere of rhenium prior to the rate-controlling step (RCS). The actual entry of PPh_3 into the cycle occurs in a fast step later in the catalytic cycle, after the RCS; its relative rate constants (k_4) were evaluated with pairwise combinations of phosphines. Substituent effects were studied in three ways: for $(YC_6H_4)_3P$, a Hammett correlation of k_c against 3σ gives the reaction constant $\rho_c^P = +1.03$, consistent with phosphine predissociation; for PyO $\rho_c^N = -3.84$. It is so highly negative because PyO enters in three steps, each of which is improved by a better Lewis base or nucleophile, and again for $(YC_6H_4)_3P$ as regards the k_4 step, $\rho_4 = -0.70$, reflecting its role as a nucleophile in attacking a postulated dioxorhenium(VII) intermediate. The RCS is represented by the breaking of the covalent N–O bond within another intermediate inferred from the kinetics, [MeReO(mtp)-$(OPy)_2$], to yield the dioxorhenium(VII) species [$MeRe(O)_2$(mtp)(OPy)]. A close analogue, [$MeRe(O)_2$(mtp)Pic], was identified by ^{1}H NMR spectroscopy at 240 K in toluene-d_8. The role of the "second" PyO in the rate law and reaction scheme is attributed to its providing nucleophilic assistance to the RCS. Addition of an exogenous nucleophile (tetrabutylammonium bromide, Py, or Pic) caused an accelerating effect. When Pic was used, the rate law took on the new form $v = k_{NA}[\mathbf{1}][\mathrm{PicO}][\mathrm{Pic}][\mathrm{PPh_3}]^{-1}$; $k_{NA} = 2.6 \times 10^2$ L mol^{-1} s^{-1} at 25.0 °C in benzene. The ratio k_c/k_{NA} is 58, consistent with the Lewis basicities and nucleophilicities of PicO and Pic.

Introduction

Oxygen atom transfer (OAT) reactions mediated by transition metals hold great interest in biological systems, organic synthesis, and industrial processes. The Mo and W atoms in oxotransferase enzymes exist in high oxidation states, Mo(VI) and Mo(IV), participating in these reactions as $Mo^{VI}(O)_2$ and $Mo^{IV}O$ species.[1−7] Molybdenum[1−3,8−10] and tungsten[11−13] compounds have been the most extensively studied. One of the key compounds was identified directly by FABMS, $L_1Mo(O)(OPPh_3)$ from $L_1Mo^{VI}(O)_2$ and PPh_3, prior to release of Ph_3PO.[10]

Important work on rhenium catalysis of OAT precedes ours;[14] we have concentrated on rhenium-catalyzed OAT reactions with oxygen acceptors such as H_3PO_2 and PPh_3.[15−17]

* To whom correspondence should be addressed. E-mail: espenson@iastate.edu.

(1) Baird, D. M.; Aburri, C.; Barron, L. S.; Rodriguez, S. A. *Inorg. Chim. Acta* **1995**, *237*, 117−122.
(2) Caradonna, J. P.; Reddy, P. R.; Holm, R. H. *J. Am. Chem. Soc.* **1988**, *110*, 2139−44.
(3) Hille, R. *Chem. Rev.* **1996**, *96*, 2757−2816.
(4) Holm, R. H.; Berg, J. M. *Acc. Chem. Res.* **1986**, *19*, 363−70.
(5) Holm, R. H. *Chem. Rev.* **1987**, *87*, 1401−49.
(6) Li, H.; Palanca, P.; Sanz, V.; Lahoz, L. *Inorg. Chim. Acta* **1999**, *285*, 25−30.
(7) Lu, X.; Sun, J.; Tao, X. *Synthesis* **1982**, 185.
(8) Laughlin, L. J.; Young, C. G. *Inorg. Chem.* **1996**, *35*, 1050−8.
(9) Smith, P. D.; Millar, A. J.; Young, C. G.; Ghosh, A.; Basu, P. *J. Am. Chem. Soc.* **2000**, *122*, 9298−9299.
(10) Smith, P. D.; Slizys, D. A.; George, G. N.; Young, C. G. *J. Am. Chem. Soc.* **2000**, *122*, 2946−2947.
(11) Johnson, M. K.; Rees, D. C.; Adams, M. W. W. *Chem. Rev.* **1996**, *96*, 2817−2839.
(12) Sung, K.-M.; Holm, R. H. *Inorg. Chem.* **2000**, *39*, 1275−1281.
(13) Sung, K.-M.; Holm, R. H. *J. Am. Chem. Soc.* **2001**, *123*, 1931−1943.

10.1021/ic0112995 CCC: $22.00 © 2002 American Chemical Society
Published on Web 03/21/2002

Chart 1

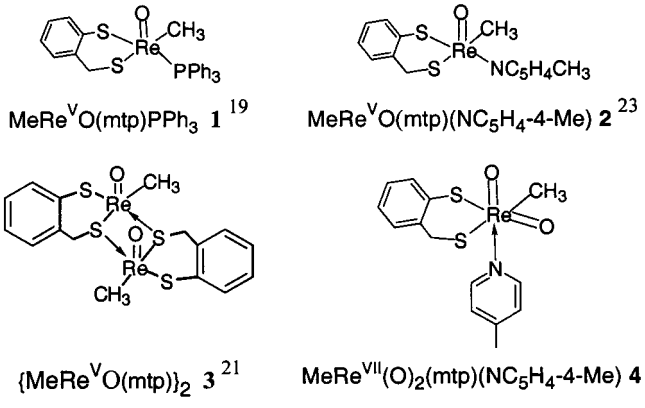

The stoichiometric oxidizing agents include, for example, pyridine *N*-oxides or, astonishingly, the normally inactive aqueous perchlorate ion. The resting state of the MTO catalyst contains Re(VII), the active or transient state, Re(V). The latter species is $MeRe^{V}(O)_2(H_2O)_n$ (perhaps $n = 2$),[17,18] a reactive but metastable compound in solution that had earlier been isolated as phosphine (PZ_3) derivatives, $MeRe(O)_2(PZ_3)_2$.[19] The poor stability of hydrated $MeRe(O)_2$ limits its utility in solution, however, as does its slow regeneration from MTO. Thus, the MTO-based catalytic system demonstrated the principle, but it is not amenable either to practical catalysis or to a clear delineation of the step-by-step elementary reactions and their mechanisms.

It seemed useful to explore a system that would reverse the roles of the resting state and transient states of the catalyst, as this might prove more useful in studies of the kinetics and mechanism. Some members of a recently synthesized series of oxorhenium(V) compounds with dithiolate ligands[20−23] have thus been explored. Among them is $MeReO(mtp)PPh_3$ (**1**) (see Chart 1). At a trace level it catalyzes OAT from pyridine *N*-oxides to phosphines on gram scales.[24] In addition the study of this OAT reaction[7,25] has been useful in the concurrent study of the mechanism.

A study of the mechanism of this reaction in particular is warranted, because it occurs without apparent side effects and **1** is an efficient catalyst for it. Moreover, the deoxygenation of heteroaromatic *N*-oxides is an important step in the synthesis of heterocycles. Many of the known methods for deprotection of pyridines[26−30] are limited by side reactions or by reduction of the ring substituents, and some require tedious procedures. This method offers a promising alternative.[24] Certain oxomolybdenum compounds catalyze the same transformation; indeed, some pyridine *N*-oxides are enzymatic substrates.[1,2,6] Our study includes a formal kinetics investigation, the design of a suitable reaction scheme, the exploration of chemical mechanisms to one or more steps, and the identification, to the extent allowed, of the intermediates involved.

Experimental Section

Materials. Methyltrioxorhenium(VII), CH_3ReO_3 or MTO, was prepared from sodium perrhenate and tetramethyltin (Strem Chemicals).[31] Compound **1** of Chart 1 and its analogues with different phosphine ligands were synthesized from MTO and $mtpH_2$, 2-(mercaptomethyl)thiophenol.[20] Full characterization was given earlier, and we cite only the characteristic ^{31}P chemical shifts in C_6D_6 for $MeReO(mtp)P(C_6H_4\text{-}4\text{-}R)$, δ/ppm: 24.7 (R = OMe), 26.5 (Me), 27.8 (H), 25.5 (F), 26.5 (Cl), and 27.3 (CF_3).

Other reagents were purchased from commercial sources and used without further purification. The generic symbols PyO and PZ_3 will be used for the general case, and PicO will be used for the most extensively studied compound, 4-picoline *N*-oxide. Solutions for kinetics measurements were prepared in benzene (Fisher Spectranalyzed) and thermostated at 25.0 °C. Deuterated benzene was the solvent for NMR kinetics measurements at 298 K. Some NMR measurements were carried out at 240 K in toluene-d_8.

Instrumentation. Shimadzu scanning spectrophotometers were used to record UV−vis spectra and the progress curves for kinetics in cuvettes with a 1 cm optical path. The reaction progress was monitored from the intensity of the pyridine *N*-oxide absorption at 330−360 nm; e.g., PicO has $\epsilon_{330} = 948$ L mol^{-1} cm^{-1}. A Bruker DRX-400 MHz spectrometer was used to obtain the ^1H and ^{31}P NMR spectra. The ^1H chemical shifts reported here were measured relative to the residual ^1H resonance of the deuterated solvent. The chemical shifts for the ^{31}P spectra were automatically referenced to that of 85% H_3PO_4 by the spectrometer.

Kinetics. Initial rates were obtained by converting absorbances to PyO concentrations, here designated *C*, according to eq 1. The concentration−time curves were fit with the least-squares program KaleidaGraph to a fifth-order polynomial. The value of the leading coefficient of the polynomial, m_1 of eq 2,

$$[PyO]_t = [PyO]_0 \frac{Abs_t - Abs_\infty}{Abs_0 - Abs_\infty} \quad (1)$$

$$[PyO]_t = [PyO]_0 - m_1 t - m_2 t^2 - m_3 t^3 - m_4 t^4 - m_5 t^5 \quad (2)$$

gives the initial rate v_i (mol L^{-1} s^{-1}) to an estimated precision of ±15%.[32] A full time-course analysis was applied to the experimental progress curves in many other experiments. These reactions

(14) Arias, J.; Newlands, C. R.; Abu-Omar, M. M. *Inorg. Chem.* **2001**, *40*, 2185−2192.
(15) Abu-Omar, M. M.; Espenson, J. H. *Inorg. Chem.* **1995**, *34*, 6239−6240.
(16) Abu-Omar, M. M.; Appleman, E. H.; Espenson, J. H. *Inorg. Chem.* **1996**, *35*, 7751−7757.
(17) Eager, M. D.; Espenson, J. H. *Inorg. Chem.* **1999**, *38*, 2533−2535.
(18) Espenson, J. H.; Yiu, D. T. Y. *Inorg. Chem.* **2000**, *39*, 4113−4118.
(19) Lahti, D. W.; Espenson, J. H. *J. Am. Chem. Soc.* **2001**, *123*, 6014−6024.
(20) Jacob, J.; Lente, G.; Guzei, I. A.; Espenson, J. H. *Inorg. Chem.* **1999**, *38*, 3762−3763.
(21) Jacob, J.; Guzei, I. A.; Espenson, J. H. *Inorg. Chem.* **1999**, *38*, 1040−1041.
(22) Lente, G.; Guzei, I. A.; Espenson, J. H. *Inorg. Chem.* **2000**, *39*, 1311−1319.
(23) Lente, G.; Jacob, J.; Guzei, I. A.; Espenson, J. H. *Inorg. React. Mech.* **2000**, *2*, 169−177.
(24) Wang, Y.; Espenson, J. H. *Org. Lett.* **2000**, *2*, 3525−3526.
(25) Huang, R.; Espenson, J. H. *J. Mol. Catal. A: Chem.* **2001**, *168*, 39−46.
(26) Konwar, D.; Boruah, R. C.; Sandhu, J. S. *Synthesis* **1990**, 337−9.
(27) Ochiai, E. *Aromatic Amine Oxides*; Elsevier: New York, 1967.
(28) Rosenau, T.; Potthast, A.; Ebner, G.; Kosma, P. *Synlett* **1999**, *6*, 623.
(29) Sim, T. B.; Ahn, J. H.; Yoon, N. M. *Synthesis* **1996**, 324−6.
(30) Trost, B. M.; Fleming, L. *Compr. Org. Synth.* **1991**, *8*, 390.
(31) Herrmann, W. A.; Kratzer, R. M.; Fischer, R. W. *Angew. Chem., Int. Ed. Engl.* **1997**, *36*, 2652−2654.
(32) Hall, K. J.; Quickenden, T. I.; Watts, D. W. *J. Chem. Educ.* **1976**, *53*, 493. This is an objective method of finding the initial rate that expresses concentrations by a power series in *t*. Typically five powers to *t* are used. The coefficient of the leading (t^1) term gives the initial rate. The precision cannot be considered as any better than 15%.

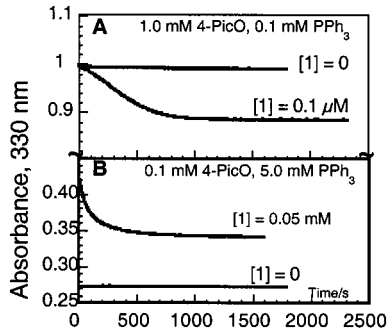

Figure 1. The decrease in the absorbance of PicO with the specified initial concentrations shows the efficiency of catalyst **1**, even at a concentration as low as 1×10^{-7} M, and the lack of reaction without **1**. In the lower panel, the initial absorbances are different because **1** itself absorbs at this wavelength.

followed pseudo-second-order kinetics with respect to the concentration of pyridine *N*-oxide, other variables being constant. The rate equation is defined in eq 3, where the coefficient of k_ψ is 1, not 2, because a single PyO is converted to product in each catalytic cycle. Integrated forms of this equation are given in eq 4 (statistically preferable, used in nonlinear least-squares data fitting)[33] and eq 5 (the traditional reciprocal form).

$$-\frac{d[\mathrm{PyO}]}{dt} = k_\psi[\mathrm{PyO}]^2 \tag{3}$$

$$\mathrm{Abs_t} = \mathrm{Abs_\infty} + \frac{\mathrm{Abs_0} - \mathrm{Abs_\infty}}{1 + [\mathrm{PyO}]_0 k_\psi t} \tag{4}$$

$$\frac{1}{\mathrm{Abs_t} - \mathrm{Abs_\infty}} = \frac{1}{\mathrm{Abs_0} - \mathrm{Abs_\infty}} + \left(\frac{k_\psi[\mathrm{PicO}]_0}{\mathrm{Abs_0} - \mathrm{Abs_\infty}}\right)t \tag{5}$$

Results

General Observations. PicO and PPh_3 were used in the first investigations. The net reaction is

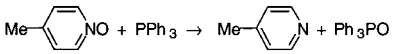

(6)

This is a spontaneous reaction, with $\Delta H°$ (and, approximately, $\Delta G°$) = −266 kJ.[34] Nonetheless, control experiments with ^{1}H and ^{31}P NMR spectroscopy showed that no reaction had occurred over >10 h. The monomeric phosphine complex **1** serves as a potent catalyst for this transformation. A reaction with a 14 mM concentration of each substrate, to which 0.042 mM **1** was added, went to completion within 1 min; a second experiment with 0.1 mM PicO, 5 mM PPh_3, and 5×10^{-5} M **1** gave an easily measured rate, Figure 1B, which also shows the control. The same kinetic curves were obtained under air as under argon, showing that molecular oxygen is not involved. Neither $MeReO_3$ nor the cyclic disulfide mtp from the decomposition of **1** was detected by ^{1}H NMR spectroscopy during or after catalytic experiments, as long as PPh_3 remained. (Controls were run to validate the detection method and its sensitivity.)

(33) Espenson, J. H. *Chemical Kinetics and Reaction Mechanisms*, 2nd ed.; McGraw-Hill: New York, 1995; pp 19 and 24.
(34) Ribeiro da Silva, M. D. M. C.; Agostinha, M.; Matos, R.; Vaz, M. C.; Santos, L. M. N. B. F.; Pilcher, G.; Acree, W. E., Jr.; Powell, J. R. *J. Chem. Thermodyn.* **1998**, *30*, 869−878.

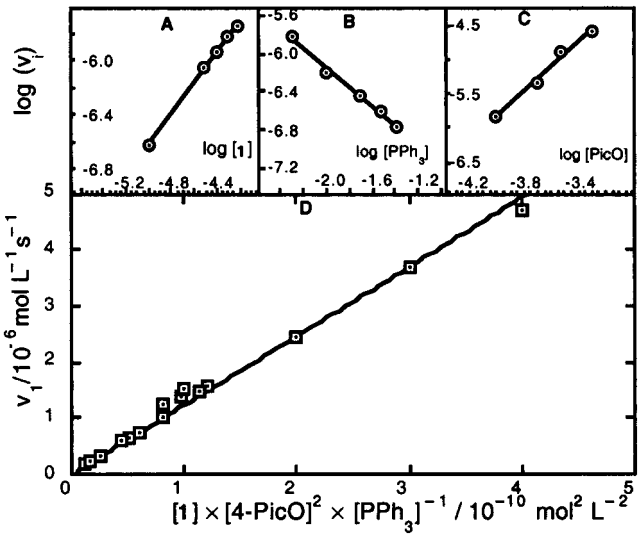

Figure 2. The initial rates of reaction depend on each concentration, as shown on log−log scales. Conditions: panel A, [**1**] was varied with 0.10 mM PicO and 5.00 mM PPh_3; panel B, [PPh_3] was varied with 0.10 mM PicO and 0.050 mM **1**; panel C, [PicO] was varied with 5.00 mM PPh_3 and 0.050 mM **1**. Panel D displays the effect of the combined concentration variable, as in eq 8.

In the absence of PPh_3, or with a deficiency, the absorbance−time profile takes on an unusual shape (Figure 1A) that may arise from the independently established decomposition reaction. The net result is given by eq 7; it likely occurs by

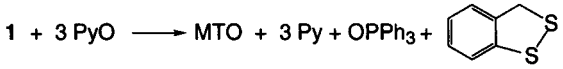

(7)

way of a particular intermediate in the catalytic cycle.

The fact that catalysis proceeds normally as long as PPh_3 remains indicates that the recycling of **1** between its resting and active states prevents its decomposition during the catalytic stage. That is, $v_{cat} \gg v_7$ when [PPh_3] > [PyO].

Initial Rate Studies, PicO + PPh_3. This method was used for the first family of experiments. Groups of experiments covering ranges of concentrations of PicO, PPh_3, and catalyst **1**, each with the other concentrations held constant, are displayed as log−log plots in Figure 2A−C (the database is given in Table S-1 in the Supporting Information). The reaction orders with respect to **1**, PyO, and PPh_3 are, respectively, 1, 2, and −1, as given by eq 8. Its form was further tested by a plot of all the values of v_i against the composite concentration variable. The data are in agreement with this model, as shown in Figure 2D.

$$-\frac{d[\mathrm{PyO}]}{dt} = k_c\frac{[\mathrm{PyO}]^2[\mathbf{1}]}{[\mathrm{PPh_3}]} \tag{8}$$

Least-squares fitting affords $k_c = (1.24 \pm 0.03) \times 10^4$ L mol^{-1} s^{-1} at 25.0 °C in benzene. The fitting error seriously underestimates the errors inherent to initial-rate kinetics; the realistic uncertainty from initial rates is more likely on the order of ±15%.

Time-Course Kinetic Analysis. Further experiments with the PPh_3 concentration in large excess over PyO were conducted to corroborate the kinetic form and rate constant

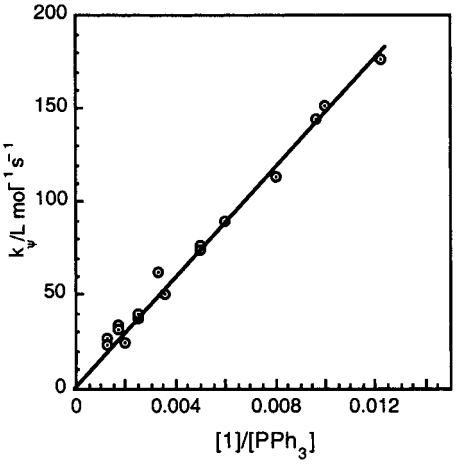

Figure 3. The pseudo-second-order rate constant for the reaction between 4-methylpyridine *N*-oxide and triphenylphosphine (in benzene at 25.0 °C) varies linearly with the ratio of the concentrations, [**1**]/[PPh_3]. The slope affords the rate constant of eq 8 as (1.50 ± 0.05) × 10^4 L mol^{-1} s^{-1}.

Table 1. Rate Constants for the Reactions between Pyridine *N*-Oxides and Triphenylphosphine, Catalyzed by MeReO(mtp)PPh_3, **1**, in Benzene at 25 °C

pyridine *N*-oxide	k_c [a]/10^3 L mol^{-1} s^{-1}	σ[b]	pyridine *N*-oxide	k_c [a]/10^3 L mol^{-1} s^{-1}	σ[b]
(4-MeO)C_5H_4NO	19.1(2)	−0.27	(2,6-Me_2)C_5H_3NO	0.0060(1)	
(4-Me)C_5H_4NO	14.9(5)	−0.17	(4-NC)C_5H_4NO	0.00404(2)	0.66
C_5H_5NO	1.22(4)	0	(4-O_2N)C_5H_4NO	0.00178(5)	0.78
(4-Ph)C_5H_4NO	0.381(3)	−0.01			

[a] The rate law $v = k_c[1][RC_5H_4NO]^2[PPh_3]^{-1}$ defines k_c. [b] σ is the Hammett substituent constant for the pyridine *N*-oxide substituent.

over the full time course. These studies used 5−40 mM PPh_3 and 0.1−0.5 mM PicO. The concentration of **1** was varied in the range 10−61 μM. From eq 2, these experiments should correspond to eq 3, where k_ψ is the pseudo-second-order rate constant; from eq 8, $k_\psi = k_c$[**1**]/[PPh_3]. The absorbance−time curves were fit to pseudo-second-order kinetics according to eq 4. The absorbance−time curves in Figures S-1 and S-2 show data for four experiments in the form of absorbance−time profiles. The data fitting was done with eq 4, not with eq 5.

Table S-2 gives the rate constant−concentration values. Figures S-3−S-5 show the functional dependences of k_ψ on [PPh_3], 1/[PPh_3], and [**1**]. The combined fit of k_ψ against [**1**]/[PPh_3], shown in Figure 3, proves to be a straight line that extrapolates to the origin. Its slope gives k_c = (1.50 ± 0.05) × 10^4 L mol^{-1} s^{-1}, where the error is the uncertainty of the fit. We assess the experimental precision to be perhaps 5%, and so k_c values from initial-rate and time-course methods are in acceptable agreement.

Kinetics with Ring-Substituted Substrates. (a) PyO. Several variations were explored. In the first, a series of substituted pyridine *N*-oxides was used with PPh_3 and catalyst **1**. The value of k_c was obtained for each reaction, according to the methods previously described. For the series of pyridine *N*-oxides, the rate constants (given in Table 1) show a strikingly large effect of the group R, spanning a factor >3 × 10^3, favoring the most electron-donating groups.

(b) P(C_6H_4R)$_3$. For the variation of phosphine substituents, different PZ_3 substrates were used in conjunction with the catalysts MeReO(mtp)(PZ_3),[35] giving the values of k_c in Table 2. Reversing the trend for the pyridine *N*-oxides, the fastest-reacting phosphines are those with the most-electron-attracting substituent, R = CF_3, and vice versa. Further analysis is deferred to the Interpretation and Discussion.

Table 2. Rate Constants for Rhenium-Catalyzed Reactions between 4-MeC_5H_4NO and Various Phosphines in Benzene at 25 °C

phosphine, PZ_3	k_c[b]/ 10^3 L mol^{-1} s^{-1}	k_c[c]/ 10^3 L mol^{-1} s^{-1}	k_4(rel)
P(C_6H_4-4-OMe)$_3$	1.93(2)	2.94(3)	6.30
P(C_6H_4-4-Me)$_3$	2.92(4)	2.43(1)	2.84
P(C_6H_5)$_3$	14.9(5)	14.9(5)	(1.000)
P(C_6H_4-4-F)$_3$	58.8(1)	24.5(1)	0.55
P(C_6H_4-4-Cl)$_3$	99.4(3)	117(1)	0.44
P(C_6H_4-4-CF_3)$_3$	477(6)	276(4)	0.11
$PMePh_2$	16.2(5)		3.11
PCy_2		0.40(1)	

[a] The rate law $v = k_c[\mathbf{1}][RC_5H_4NO]^2[PPh_3]^{-1}$ defines k_c; the uncertainties are the errors of the fitting. [b] The catalyst is MeReO(mtp)PZ_3; our analysis indicates this column of values is the more reliable in describing the effect on catalytic reactivity. [c] The catalyst is **1**, MeReO(mtp)PPh_3.

Scheme 1. Skeleton Reaction Scheme

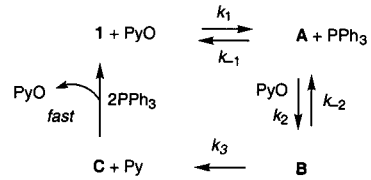

Skeleton of the Reaction Scheme. It proved helpful to construct a tentative outline of the reaction scheme based on the data presented to this point, as given in Scheme 1. In brief, it comprises the following steps: (1) **1** and PyO form the first Re-containing intermediate **A**, releasing PPh_3; (2) a second PyO adds to **A**, forming a second intermediate, **B**; (3) pyridine is released from **B**, to form a third intermediate, **C**; (4) **C** reacts with PPh_3, returning to **1** (likely in more than one step) quite rapidly, without an influence on the rate.

The rate law for Scheme 1 was derived, as given in the Supporting Information. Equation 9 was obtained when the steady-state approximation was made for the concentrations of the intermediates. To attain correspondence between it and eq 8, the PyO denominator term in eq 9 must be negligible, so that the equation simplifies to the first form in eq 10. The chemical sense of the scheme as well as other data gives $k_3 \ll k_{-2}$, allowing further simplification to the second form in eq 10.

$$v = -\frac{d[PyO]}{dt} = \frac{k_1k_2k_3[\mathbf{1}][PyO]^2}{k_2k_3[PyO] + (k_{-1}k_3 + k_{-1}k_{-2})[PPh_3]} \quad (9)$$

$$v = -\frac{d[PyO]}{dt} = \frac{k_1k_2k_3[\mathbf{1}][PyO]^2}{(k_{-1}k_3 + k_{-1}k_{-2})[PPh_3]} \cong K_1K_2k_3\frac{[\mathbf{1}][PyO]^2}{[PPh_3]} \quad (10)$$

(35) Another set of experiments used **1** as the catalyst with different PZ_3 substrates, but ligand exchange during catalysis made these data less useful; they are, however, also included in Table 2.

Scheme 2. Partitioning between Phosphine Oxides

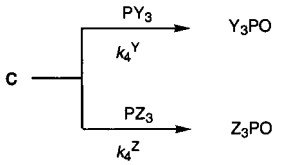

Further experiments were then planned to amplify this model: kinetics studies at another extreme of the concentration variables, [PicO] ≫ [PPh_3], in an effort to reduce eq 9 to a different limiting form, competition experiments to determine the rate constants for step 4 of Scheme 1, tests of the postulated role of PyO in step 2 with an alternative nucleophile to assist in the elimination of pyridine, which we believe to be the chemical importance of the rate-controlling step (RCS), step 3, and the explicit detection of **4**, a close analogue of intermediate **C**, with Pic instead of PicO.

Kinetics with [PicO] ≫ [PPh_3]. The reaction became extremely rapid at this concentration limit, because of the second-order dependence on the one and the inverse dependence on the other. The catalyst concentration was lowered to $(1-5) \times 10^{-7}$ M; catalysis continued. The reaction then showed a first-order dependence on [PicO] (Figure S-6). The rate law under these conditions takes a different limiting form of eq 9, as given by eq 11.

$$v = k_1[\mathbf{1}][\mathrm{PicO}] \tag{11}$$

Experiments carried out under these conditions give the rate constant for the first step, $k_1 = (9.6 \pm 0.3) \times 10^2$ L mol^{-1} s^{-1}. Without a greater amount of PPh_3, the decomposition of **1** (eq 7) and its entry into the first part of the catalytic cycle (Scheme 1, k_1 step) occur concurrently.

Competition Kinetics for Intermediate C. Step 4 of Scheme 1 must take place after the RCS to be in accord with the kinetics. Thus, the kinetics of any given phosphine will not provide information about the k_4 step. An experiment using a pair of phosphines can do so, however, as shown in Scheme 2. The partitioning of the two phosphines to their respective oxides is governed not by the net reaction kinetics, but by the relative rate constants of the k_4 step, however high they may be in comparison with the rate constants of the other steps.

Dividing the rates of phosphine loss gives an equation from which [**C**] cancels:

$$\frac{v_4^{\mathrm{Y}}}{v_4^{\mathrm{Z}}} = \frac{\mathrm{d}[\mathrm{PY}_3]}{\mathrm{d}[\mathrm{PZ}_3]} = \frac{k_4^{\mathrm{Y}}[\mathrm{PY}_3][\mathbf{C}]}{k_4^{\mathrm{Z}}[\mathrm{PZ}_3][\mathbf{C}]} \tag{12}$$

Integration yields an equation that can be cast in linear form, the final term in eq 13 being a constant in each experiment.

$$\ln\{[\mathrm{PY}_3]_t\} = \left(\frac{k_4^{\mathrm{Y}}}{k_4^{\mathrm{Z}}}\right)\ln\{[\mathrm{PZ}_3]_t\} - \left(\frac{k_4^{\mathrm{Y}}}{k_4^{\mathrm{Z}}}\right)\ln\left\{\frac{[\mathrm{PZ}_3]_0}{[\mathrm{PY}_3]_0}\right\} \tag{13}$$

To provide sufficient time resolution for careful measurements of phosphine concentrations by ^{31}P and ^{1}H NMR spectroscopies, we chose to use the slowly reacting PyO, 2-methyl-4-nitropyridine *N*-oxide, even though it was not used as a substrate in catalytic kinetics. [Note, however, that the choice of PyO is immaterial as regards the determination of k_4(rel), aside from specifying the time scale for phosphine oxide buildup.] With this PyO the overall reaction now required >10 h to reach completion. The data from two competition experiments are shown in Figure 4. The slopes of the lines of the double-logarithmic plots gave the ratio of two rate constants. Values of k_4 referenced to PPh_3 ($k_4^{\mathrm{H}} = 1.000$) are given in Table 2.

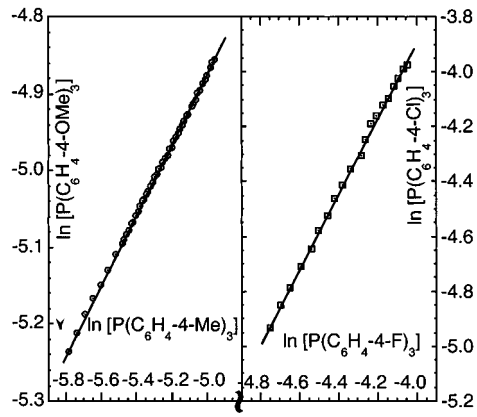

Figure 4. Data from competition experiments at 25 °C in C_6D_6 on the reaction of 2-methyl-4-nitropyridine *N*-oxide (PyO) with pairs of phosphines. Data are plotted in the double logarithmic form of eq 14; the rate constant ratio is given by its slope. The concentrations in panel A were 10 mM $P(C_6H_4\text{-}4\text{-}OMe)_3$, 10 mM $P(C_6H_4\text{-}4\text{-}Me)_3$, 20 mM PyO, and 0.5 mM **1**; those in panel B were 20 mM $P(C_6H_4\text{-}4\text{-}Cl)_3$, 20 mM $P(C_6H_4\text{-}4\text{-}F)_3$, 32 mM PyO, and 0.5 mM **1**.

Alternative Nucleophilic Assistance. We will argue that the "second" PicO entering in the k_2 step of Scheme 1 does so to provide nucleophilic assistance to the breaking of the covalent O−Pic bond of the "first" PicO group, at that point coordinated to rhenium. If so, then an alternative second nucleophile may substitute for it. This was tested with Py, Pic, and tetrabutylammonium bromide. These reagents exert the predicted accelerating effect, as shown in Figure 5, but do not undergo a net *or transient* conversion during the process, save that a very small fraction may temporarily coordinate to rhenium.

This subject was made quantitative for Pic. If its role at this stage is as suggested, then the rate law can be written as

$$v = (k_c[\mathrm{PicO}] + k_{\mathrm{NA}}[\mathrm{Pic}])\frac{[\mathbf{1}][\mathrm{PicO}]}{[\mathrm{PPh}_3]} \tag{14}$$

where the added term k_{NA}[Pic] represents the effect of Pic. Experiments were carried out with 0.050 mM **1**, 10 mM PPh_3, 2−8 mM Pic, and 0.10 mM PicO. The use of [Pic] ≫ $[\mathrm{PicO}]_0$ was our effort to make the second term the predominant one. Indeed, the kinetic data from these experiments were well fitted by pseudo-first-order kinetics; Figure S-7. The plot of k_ψ against [Pic] was linear (Figure S-8) according to the relation

$$k_\psi\frac{[\mathrm{PPh}_3]}{[\mathbf{1}]} = k_c[\mathrm{PicO}] + k_{\mathrm{NA}}[\mathrm{Pic}] = 3.2 \times 10^{-3} + (2.6 \times 10^2)[\mathrm{Pic}] \tag{15}$$

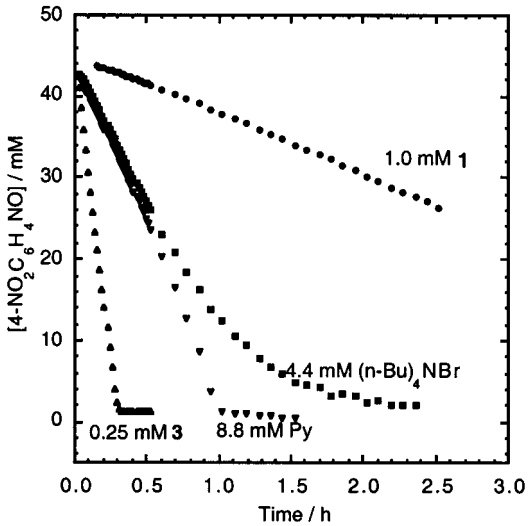

Figure 5. Disappearance of 44.4 mM 2-methyl-4-nitropyridine *N*-oxide in solutions with 44.4 mM PPh_3, with catalyst **1** by itself, and with assistance from two nucleophilic reagents. Also illustrated is the fact that the dimer **3** is a considerably more active catalyst than **1**.

From the slope, one finds that $k_c/k_{NA} = 58$, implying that PicO is that much more efficient than Pic in assisting this critical step. PicO is not without a residual effect, however, represented by the intercept. Its value can be compared to what is expected from the leading term in eq 14; as an approximation, we estimated the intercept using $[PicO]_{1/2} = 5 \times 10^{-5}$; thus $k_c[PicO]_{1/2}[\mathbf{1}]/[PPh_3] = 3.8 \times 10^{-3}\ s^{-1}$, in agreement with experiment given the nature of this treatment.

Detection and Characterization of Dioxorhenium(VII). No such species was observed in the direct reaction between **1** and PicO, eq 7. One reason may be that phosphines are such strong Lewis bases stabilizing **1** that any $Re^{VII}(O)_2$ would be at a concentration too low to detect, limited by the very low rate of phosphine displacement from **1**. We therefore changed to **2**, with a Pic ligand that is much more labile[19,22] and much less tightly coordinated (the reaction **1** + $C_5H_5N \rightarrow$ **2** + PPh_3 has $K_{298} = 1.1 \times 10^{-3}$ in benzene.[22]) Upon addition of 4 mM PicO to 4 mM **2** containing 20 mM excess Pic, a red compound believed to be **4** was immediately and quantitatively formed at 240 K in toluene-d_8. Peak integration relative to an internal standard showed that an additional 4 mM concentration of free Pic was formed. With 2 mM PicO, only 2 mM **4** was formed; with 8 mM PicO, 4 mM **4** resulted along with MTO and mtp from decomposition. The NMR spectrum of **4**, presented in Figure 6, allows us to assign the following resonances to **4**: δ/ppm 3.99 (s, 3H, Re−CH_3), 4.38 (d, 1H, $J = 12$ Hz), 4.11 (d, 1H, $J = 12$ Hz), 1.96 (s, 3H), 6.51(d, 2H, $J = 4$ Hz), 6.6−7.0 (m, 4H), 8.08 (d, 2H, $J = 4$ Hz). Attempts to isolate **4** failed, and only the final products of eq 7 could be obtained. When held at 240 K, **4** finally decomposed to MTO, mtp, and minor unidentified species.

Further evidence identifying **4** was obtained from reactions between **2** and (separately) *tert*-butyl hydroperoxide, dimethyl sulfoxide, and PyO at 240 K, all of which formed the same **4**.

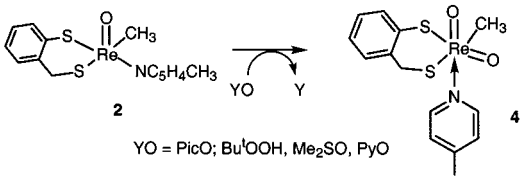

(16)

When 4-*tert*-butylpyridine was added to **4** at 240 K, a ligand exchange reaction occurred. The pyridine ligand of **4** is labile, and two pyridines compete for one coordination site:

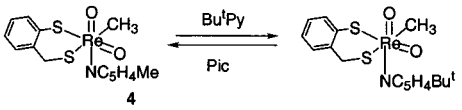

(17)

Addition of 4 mM PPh_3 to 4 mM **4** in a Pic-containing solution at 240 K gave formation of Ph_3PO, although the

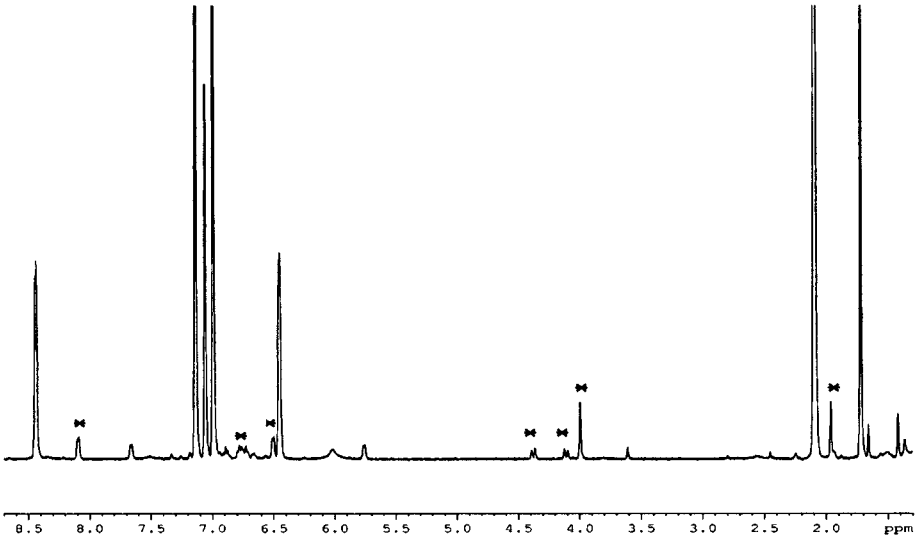

Figure 6. ^1H NMR spectrum of a solution of compound **4** taken immediately after 3 equiv of PicO was added to a solution containing 4 mM compound **2** and 20 mM Pic in toluene-d_8 at 240 K. Resonances belonging to compound **4** (*): δ/ppm 1.96 (s, 3H), 3.99 (s, 3H), 4.11 (d, 1H, $J = 12$ Hz), 4.38 (d, 1H, $J = 12$ Hz), 6.51(d, 2H, $J = 4$ Hz), 6.6−7.0 (m, 4H), 8.08 (d, 2H, $J = 4$ Hz). Other resonances in this spectra belong to 4-picoline, δ/ppm 1.73 (s, 3H), 8.46 (d, 2H, $J = 4$ Hz), 6.47 (d, 2H, $J = 4$ Hz); 4-picoline *N*-oxide, δ/ppm 1.42 (s, 3H), 5.75 (d, 2H, $J = 4$ Hz), 7.66 (d, 2H, $J = 4$ Hz); and residual ^1H resonances of toluene-d_8, δ/ppm 2.09 (m), 6.98 (m),7.00 (m), 7.09 (m). The small resonance at δ 3.62 was independently confirmed to be the cyclic disulfide from the oxidation of the mtp ligand, which occurred only to a small extent.

Scheme 3. PicO Stabilizes the Dimer against Py Monomerization Reaction

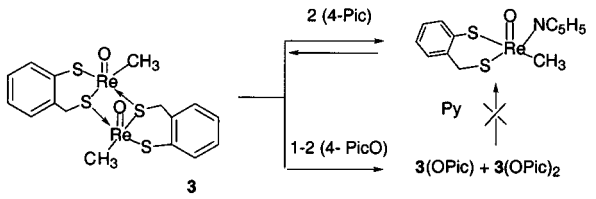

reaction remained incomplete after 10 min. But with 4 mM PicO present from the start, Ph_3PO was formed quantitatively and immediately (<1 min).

Catalysis by {MeReO(mtp)}$_2$. Dimeric **3** is an even better catalyst than **1**. This was shown in experiments that used the sluggish but convenient substrate 2-methyl-4-nitropyridine *N*-oxide. The rate acceleration of **3** over **1**, shown in Figure 5, amounts to a factor of ca. 90 per mole of catalyst, or 45 per Re atom. In ^{1}H NMR experiments at 240 K, coordination of 0.8−15.2 mM PicO to 2.0 mM **3** could be detected, showing two compounds (only) with 1:1 and 1:2 ratios of PicO. They and **3** equilibrate so rapidly even at 240 K that individual spectra could not be resolved, as reported previously.[22] A stack plot of NMR data is shown in Figure S-9.

Although PicO coordinates to dimer **3**, the coordination does not lead to the monomerization reactions that are well established for pyridines and other ligands.[22] Instead the **3**(OPic) and **3**(OPic)$_2$ adducts remain, even when Py is added; i.e., Py does not convert the adducts to **2** (Scheme 3). At longer times, decomposition analogous to eq 7 sets in, resulting in MTO and the disulfide of mtp.

Interpretation and Discussion

Reaction Scheme and Chemical Mechanism. On the basis of kinetic and spectroscopic data, thermodynamic affinities, and the detection of intermediates, Scheme 4 can be proposed. It comprises several steps, many of which are well-known ligand displacement reactions of MeReO(mtp)L.[19,22] The only step that is not ligand displacement is the one with the rate constants k_3 and k_4, to which particular attention will be paid.

Comparing Schemes 2 and 4, we note the following assignments: **A** is **5**, **B** is **6**, and **C** is a composite of **7** and species involved in its subsequent reactions. The first step represents ligand substitution.[19,22] It is unfavorable, because **1** can be detected during catalysis, but not **5**. The replacement of PPh_3 by C_5H_4N is not spontaneous with an equilibrium constant of 1.1×10^{-3}.[22] Noting qualitatively that PicO is a somewhat better Lewis base than Py for the Re(V) compounds, one can say $pK_1 < 3$.

The second step in Scheme 4 represents the formation of the bis(PyO) complex **6**. Examples of MeReO(mtp)L$_2$ have not been reported for a monodentate ligand L, and one can presume that its formation constant K_2 will be small. The coordination of a ligand trans to the oxo group is disfavored by the formation of p_π–d_π oxo−rhenium bond(s), and the step between **5** and **6** is expected to be a rapidly established equilibrium favoring **5**. On the other hand, it is only reasonable that some MeReO(mtp)(OPic)$_2$ should form, given known six-coordinate complexes of bidentate ligands (e.g., 2,2′- bipyridine, 1,10-phenanthroline, and *o*-bis(diphenylphosphino)benzene).[36] It is reasonable to make the steady-state approximation for **6**, as it remains a minor but reactive species during the catalytic cycle.

The unimolecular severing of the covalent O−N bond of PyO is represented in Scheme 4 by the conversion of **6** to **7**, with rate constant k_3. This is believed to be the RCS, rather than step 2, although either assignment would be consistent with the formal kinetics. Weak coordination to the lower axial position of **1** is quite rapid. A persuasive argument can be made for assigning k_3 as the key rate constant for the RCS, as one can infer from the reasoning given in the preceding paragraphs. In step 3, the Re(V) intermediate **6** is oxidized to Re(VII) **7**, as PyO is reduced to Py. This step is strongly influenced by the second PyO, which we attribute to *nucleophilic assistance*. Figure 5 shows the accelerating effect of exogenous nucleophiles (tetrabutylammonium bromide and pyridine). The following diagram, in which the d^2

Scheme 4. Chemical Reaction Scheme

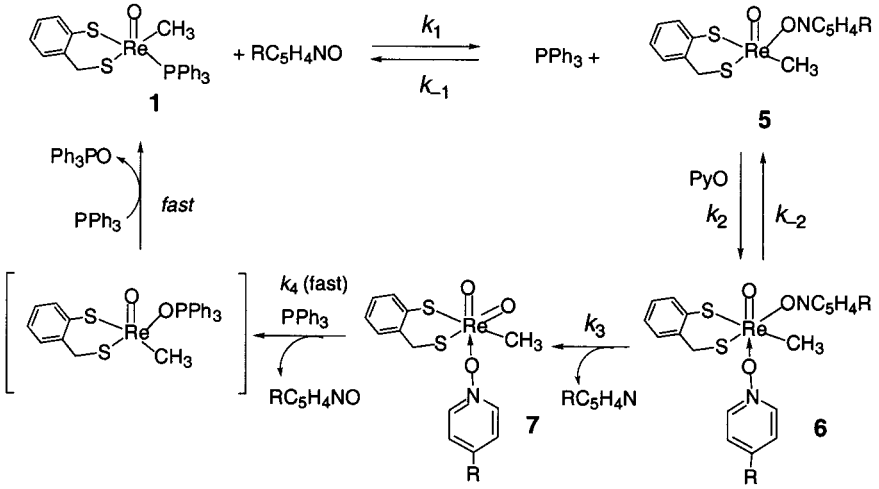

Table 3. Rate Constants for Selected Reactions of Dioxo Complexes of Rhenium(VII) and Molybdenum(VI) with Nucleophiles

dioxo reagent[a]	PZ_3	solvent	k_{298}/ L mol^{-1} s^{-1}	ref
$MeRe^{VII}(O)_2(OPic)$	PPh_3	benzene	$>10^3$	this work
$L^1Mo^{VII}(O)_2$	PEt_3	DMF	5.6×10^{-3}	38
$L^2Mo(O)_2$	PPh_3	DMF	7×10^{-3}	39
$L_2{}^3Mo(O)_2$	PPh_3	benzene	0.19×10^{-3}	40
$[L^4MoO_2(S_2PPr^i{}_2)]^-$	PPh_3	toluene	0.25×10^{-3}	19, 22
$[Re(O)_2(hoz)_2]^+$	PhS(O)Me	CD_3CN	$(1.0(4) \times 10^{-3}$, 23 °C)[b]	14

[a] Ligands are identified in ref 41. [b] From the admittedly imprecise intercept of their Figure 3.

electrons of Re(V) are explicitly shown, demonstrates how we envisage this step:

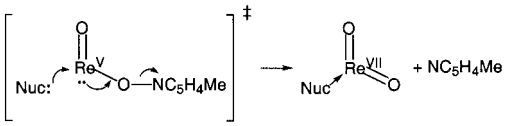

The catalytic cycle is completed in the step represented by the rate constant k_4. The chemistry is well-known: for example, phosphines *slowly* abstract an oxygen atom from MTO, $PPh_3 + MeReO_3 \rightarrow Ph_3PO + MeReO_2$.[17,37] The rhenium−oxygen bonds of MTO are strong; an estimate based on kinetics gave $\Delta G° \approx 234$ kJ for $MeReO_3(aq) \rightarrow MeRe(O)_2(H_2O)_2 + O_2(g)$ in aqueous solution.[16] A much different situation must prevail for **7**, however, as it reacts with phosphines rapidly; it was characterized by competition kinetics. A comparison for **7** might be provided by the metastable compound that was identified in solution, $[Re(O)(hoz)_2]^+$, where hozH = 2-(2′-hydroxyphenyl)-2-oxazoline.[14] It has $\Delta G° \cong 96$ kJ, much less than the analogous value for $MeReO_3$; both refer to $Re^{VII}(O)_2 \rightarrow Re^{V}O + 0.5O_2$. By means of the competition experiments described, it was possible to determine the *relative* values of k_4 for a representative selection of phosphines. Little more than a guess, we estimate $k_4{}^H > 10^3$ L mol^{-1} s^{-1}.

Certain comparison compounds[14,38,39] come to mind, as presented in Table 3. These data substantiate that the rhenium catalysts are in general much more active than the molybdenum ones as regards the step $M(O)_2 \rightarrow M(O)$. The same appears true of the overall catalytic conversion, despite the need for the predissociation of a phosphine ligand when catalysts such as **1** are used.

Reactivity Trends and Hammett Correlations. The effects of ring substituents on three different components of the experimental data were determined. It has been found that ring substituents on triarylphosphines exert opposing

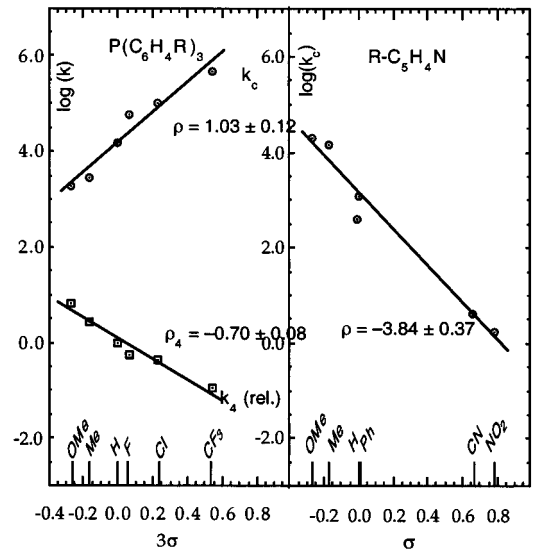

Figure 7. Analysis of the kinetic effects of pyridine *N*-oxide (right) and phosphine para substituents on the rate constants by the Hammett equation, showing log(k) against 3σ (PAr_3) or σ (PyO).

effects on the catalytic rate constant and the kinetically insignificant but product-determining rate constant k_4.

Phosphines inhibit the overall catalytic OAT reactivity by mass-law retardation of step 1. This is an equilibrium phenomenon as far as its effect on the catalytic rate constant k_c goes (refer to the algebraic simplification of eq 10 to eq 11). The value of k increases with more electron-withdrawing substituents R on $P(C_6H_4R)_3$. A plot of log k_c for eq 8 vs the Hammett substituent constant σ is shown in Figure 7, $\rho_c = 1.03(12)$. Given that $k_c = K_1K_2k_3$ and phosphine involvement is in K_1 only, $\rho_c = \rho_1$. The positive reaction constant indicates the role suggested for phosphine is consistent with its assigned chemical role: in this step the weakest Lewis base gives the greatest extent of equilibrium release of phosphine.

The second mechanistic role of the phosphine is to participate in the rapid reaction represented by k_4. The fact that relative and not absolute values of k_4 were determined is immaterial as far as the validity of the LFER analysis is concerned. The Hammett analysis of these values, also presented in Figure 7, gives ρ(for k_4) $= -0.70(2)$. The negative reaction constant for the phosphines in this step illustrates it acts here as a nucleophile, attacking the oxo group of the dioxorhenium(VII) intermediate **7**.

As remarked earlier, the kinetic effect of pyridine ring substituents is quite large, with $\rho = -3.84(8)$, also shown in Figure 7. The overall reaction constant ρ(for k_c of eq 8) $= \rho_1 + \rho_2 + \rho_3 = -3.84$. The large effect arises because PyO plays the role of a Lewis base in the two equilibria and a nucleophile in the k_3 step. All three will have negative reaction constants, which accounts for the unusually large magnitude of the reaction constant ρ_c. Pyridines with ortho substituents are excluded from the Hammett analysis, but react much more slowly; k for 2,6-lutidine *N*-oxide is 10^3 times less than k for PicO. This is evidence of steric effects as well as electronic effects.

Conclusions. Scission of the covalent N−O bond of pyridine *N*-oxides takes place by a multistep mechanism that

(36) Espenson, J. H.; Shan, X.; Lahti, D. W.; Rockey, T. M.; Saha, B.; Ellern, A. *Inorg. Chem.* **2001**, *40*, 0000.
(37) Herrmann, W. A.; Roesky, P. W.; Wang, M.; Scherer, W. *Organometallics* **1994**, *13*, 4531−4535.
(38) Schultz, B. E.; Holm, R. H. *Inorg. Chem.* **1993**, *32*, 4244−8.
(39) Berg, J. M.; Holm, R. H. *J. Am. Chem. Soc.* **1985**, *107*, 925−932.
(40) Deli, J.; Speier, G. *Transition Met. Chem.* **1981**, *6*, 227−9.
(41) L^1 = bis(4-*tert*-butylphenyl)-2-pyridylmethanethiolate(−); L^2 = 2,6-bis(2,2-diphenyl-2-mercaptoethyl)pyridine(2−); L^3 = Et-L-cys = ethyl-L-cystein(−); L^4 = hydrotris(3,5-dimethylpyrazol-1-yl)borate(−); hozH = 2-(2′-hydroxyphenyl)2-oxazoline.

has been resolved into factors that combine to make this possible: (1) the inductive effect of high-valent rhenium to which PyO becomes coordinated, (2) the existence of a coordination site for the oxygen atom, (3) the assistance of either a second PyO or an exogenous nucleophile, and (4) to complete the catalytic cycle, the conversion of the oxidized Re(VII) compound (one form of which was detected directly by low-temperature NMR) back to the parent catalyst form upon reaction with phosphine. The roles assigned to these reagents are supported by the inductive effects accorded to each of three kinetic parameters from the LFER analyses.

Acknowledgment. This research was supported by the U.S. Department of Energy, Office of Basic Energy Sciences, Division of Chemical Sciences, under Contract W-7405-Eng-82.

Supporting Information Available: Tabulations and plots of kinetic data to illustrate agreement with selected mathematical forms and to evaluate numerical parameters. This material is available free of charge via the Internet at http://pubs.acs.org.

IC0112995